Kinetic Crystallization of Polypropylene in Ternary Composites Based on Fiber-Reinforced PP-EPDM Blends

MIGUEL A. LÓPEZ MANCHADO,* LUIGI TORRE, JOSÉ M. KENNY

Materials Engineering Center, University of Perugia, Loc. Pentima Bassa 21, 05100 Terni, Italy

Received 6 January 2000; accepted 24 July 2000

ABSTRACT: The crystallization of isotactic polypropylene (iPP) in its blends with ethylene–propylene–diene terpolymer (EPDM), reinforced with different fibers, is described in this work. In particular, the effects of both the fibers and the EPDM on the crystallization kinetics and morphology of iPP are analyzed. The study was performed using differential scanning calorimetry (DSC) in dynamic and isothermal conditions and optical microscopy. It was found that all the fibers act as effective nucleant agents on iPP crystallization independently of the blend composition. The results obtained highlight the accelerating effect of the fibers and of the EPDM on the PP crystallization up to a certain EPDM percentage. The halftime of crystallization, $\tau_{1/2}$, and the overall crystallization rate, K_n, increase in the presence of all the fibers analyzed, showed the aramidic ones the most effective. The isothermal crystallization kinetics of ternary composites based on PP–EPDM blend matrices reinforced with different types of fibers can be modeled using the Avrami equation. On the other hand, the kinetic curves obtained under nonisothermal conditions provide a further confirmation of the nucleating action of the fibers on the PP crystallization. Optical polarizing microscopy was also used to investigate the effect of EPDM on the spherulite growth and the transcrystallinity phenomenon on the surface of the fibers. The results of such analysis showed that the transcrystallinity phenomenon is hindered at high rubber percentages. As in the case of the rate of crystallization, the highest proportion of transcrystallinity was observed in the presence of the aramidic fibers. J Appl Polym Sci 81: 1063–1074, 2001

Key words: PP; EPDM; composites; crystallization kinetics; transcrystallinity

INTRODUCTION

Polypropylene (iPP) is the thermoplastic of higher consumption due to its well-balanced physical and mechanical properties and its easy processability at relatively low cost. However, in some cases, not all the characteristics of this material are suitable for common service conditions. For instance, the relatively high PP glass transition temperature (T_g) and its high crystallinity makes it unsuitable for low-temperature applications. It is, therefore, necessary to improve its flexibility and resilience at low temperatures.[1,2] Thus, impact modifiers can be added to PP and, among them, rubber ethylene–propylene–diene terpolymer (EPDM), due to its high impact strength over a wide temperature range is considered one of the most effective.[3–8] These blends, commonly referred to as polyolefin thermoplastic elastomers (TPOs), are a special class of thermoplastic elas-

Correspondence to: J. M. Kenny (Kenny@unipg.it).

Contract grant sponsors: Ministry of Education and Culture (Spain), and Ministery of University and Scientific Research (MURST).

* Current address: Institute of Polymer Science and Technology, Madrid, Spain.

Journal of Applied Polymer Science, Vol. 81, 1063–1074 (2001)

tomers (TPE) that combine the good processing characteristics of thermoplastics at elevated temperatures[9–11] with the physical properties of conventional elastomers at service temperatures,[12,13] playing an increasingly important role in the polymer industry.

However, the addition of the elastomeric phase gives rise to a marked decrease of some PP properties, such as stiffness and hardness, limiting its application fields. To improve these properties, considerable work has been performed on PP ternary blends. For example, it has been reported that the addition of high-density polyethylene (HDPE) to PP-elastomer blends improves the blend stiffness and the rubber dispersability.[14–16] However, only few results on ternary PP composites can be found in the literature. The main goal of the present study is to prepare and to analyze the properties of ternary composites based on PP–EPDM blend matrices reinforced with different fibers. Furthermore, it is well known that PP is one of the most used thermoplastic matrices for fiber-reinforced composites. It is, in fact, possible to obtain good composites using PP with different fibers and fillers processed with common techniques such as injection molding and compression molding.

In the study of PP composites it must be considered that the morphology of PP can be affected by the presence of the fibers. Such phenomenon can be responsible for significant modifications on the mechanical properties of the composites.[17] Moreover, if a high number of nuclei is formed at the fiber interface, the lateral development of the spherulites is obstructed, and a columnar growth or transcrystalline growth of crystals on the fiber surface takes place.[18,19] The mechanism of transcrystallization is still not fully understood; there are, in fact, no general rules to relate processing conditions to transcrystallinity and transcrystallinity to the final properties of the different fiber–matrix systems. However, it has been shown that the presence of transcrystalline regions on the fiber surface can improve the mechanical properties of some fiber-reinforced polymers.[20,21]

The study of the crystallization kinetics of polymers is of great importance for the analysis and the design of processing operations and their relation with the final polymer structure. Furthermore, the microstructure of crystallizable polymer matrices plays a very important role in the thermoplastic composite characteristics. Calorimetry may be considered as one of the most interesting and effective technique for the macrokinetic analysis of polymer crystallization.

Several studies on the crystalline morphology of the PP in PP–EPDM blends or in fiber-reinforced composites have been carried out in the last years; however, there are not many studies dedicated to investigate the microstructure and crystallinity of polymers in ternary composites.[22,23] Jancar and Dibenedetto[24] have investigated the effect of the phase morphology on the tensile yield strength of polypropylene/ethylene–propylene copolymer blends with inorganic fillers. In previous studies we have separately investigated the effect of the EPDM[25] and of the fibers[26] on the crystallization kinetics and morphology of PP. The goal of the present work is to analyze the combined effect of EPDM and fibers on the morphology of PP-based composites and to evaluate its kinetic parameters and thermodynamics characteristics. Furthermore, a comparative study between the properties of each different composite is carried out. Thus, two organic fibers (polyethylene terephthalate (PET) and aramidic), one inorganic (glass), and one vegetal fiber (sisal) were used in this work.

EXPERIMENTAL

Materials

Commercially available grades of polypropylene (iPP) generously supplied by Montell, ethylene–propylene–diene terpolymer rubber (EPDM) with 5-ethylidene-2-norborene (ENB) as a termonomer and PET, aramidic, glass, and sisal (*Agave sisalana*) fibers were used in this work. The material specifications are listed in Table I.

The composites were prepared in a Haake Rheomix 90 internal mixer equipped with a pair of high shear roller-type rotors at 190°C and for a period of time of 20 min. The rotor rate was set at 60 rpm. Once the matrices were melted, the appropriate percentage of fiber was added (20% by weight). Then, the compounds were compression molded at 200°C. Testing samples were cut from the molded plaques. Two formulations of PP–EPDM blends were analyzed (75–25% and 50–50%) in this study. The crystallization conditions used are reported in Table II.

Measurements

Thermal analysis measurements were performed using a DSC Perkin-Elmer Pyris 1 differential

Table I Physical and Mechanical Characteristics of PP, EPDM, and of the Fibers Studied

Material	iPP	EPDM	PET	Aramidic	Sisal	Glass
Manufacturer	Montell	Bayer	Velutex-Flock, S.A.	Akzo, S.A.	—	Vetrotex
Designation	C 30 G	Buna EPT 6470P	—	Twaron 1080	—	P 368
Density (g/cm^3)	0.92	0.86	1.38	1.45	1.41	2.50
Mooney viscosity ML (1 + 8) 125°C	—	55 ± 5				
Diameter (μm)			17	12	200	11
Lenght (mm)			6	6	6	5
Melt index (g/10 min)	6.0	—				
Hardness (shore A)	—	68.7				

scanning calorimeter. Crystallization tests were carried out either in isothermal conditions at different temperatures, and in dynamic conditions at several cooling rates, to cover a wide range of thermal conditions. For the isothermal testing, samples of about 8 mg were melted at 200°C for 10 min to eliminate any previous thermal history in the material. Then they were rapidly cooled to the crystallization temperature, T_c, and maintained at that temperature during the necessary time to complete the crystallization of the matrix. Seven crystallization temperatures have been examined in a range comprised between 125 and 140°C. The heat evolved during the isothermal crystallization (ΔH_c) was recorded as a function of time, at different crystallization temperatures. The experiments were carried out in nitrogen atmosphere, and after the isothermal crystallization tests a dynamic scan at 10°C/min was performed to check the presence of residual crystallinity. Plots of the degree of crystallization as a function of time were made by integrating the area under the exothermic peaks. Subsequently, the melting temperature (T_m) of the blends was calculated as the one corresponding to the maximum of the endothermic peak.

For dynamic DSC testing, samples of about 8 mg were heated from 30 to 200°C at a heating rate of 10°C/min and then kept at that temperature for 10 min to eliminate any thermal history in the material. Samples were subsequently cooled down to −50°C using six prefixed scan rates in a range from 1 to 50°C/min. After the dynamic crystallization a heating scan at 10°C/min was performed to check the presence of residual crystallinity.

The crystalline morphology of the samples was analyzed on films using an optical polarizing microscope, Leika Metalographic Aristomet, equipped with a Mettler FP-90 automatic hot-stage thermal control. Samples were sandwiched between microscope cover glasses, melted at 200°C for 10 min, and then rapidly cooled to the crystallization temperatures shown in Tables II and III. The spherulitic growth and the transcrystallinity were observed by taking photomicrographs at different intervals of time.

RESULTS AND DISCUSSION

Isothermal Crystallization

The effect of the rubbery phase on the PP crystallization rate was analyzed in a previous study.[25] It was observed that the PP crystallization rate increases in presence of the EPDM, and this increment is more evident at the lower concentration of the amorphous polymer (25%). This behavior can be observed in Figures 1 and 2, where an isothermal thermogram (Fig. 1) and the corresponding curves of the degree of crystallization (Fig. 2) of PP and PP–EPDM blends, obtained at 130°C, are represented. These complex effects of the elastomer on PP crystallization were attributed to the modification of the PP matrix superstructure by the incorporation of the rubber. Thus, a change of the average size and number of the spherulites was induced by the presence of the rubber particles, and this structural change is very important to interpret the function as impact modifier of the elastomer in the PP matrix. Moreover, the particular crystallization behavior of PP in the blend was also attributed to the role of EPDM to selectively extract defective chains from the PP in the molten state.[27]

Table II Crystallization Parameters of PP in PP–EPDM (75–25) Blend and Its Composites

Material	T_c [°C]	$\tau_{1/2}$ [s]	K_n [min-n]	n	T_m (°C)
PP-EPDM 75-25 blend matrix					
	125	60	6.93×10^{-1}	2.18	164.9
	127	97	1.85×10^{-1}	2.70	165.0
	130	178	3.23×10^{-2}	2.81	165.8
	132	275	1.13×10^{-2}	2.69	166.8
	135	627	1.38×10^{-3}	2.64	167.6
	137	958	5.07×10^{-4}	2.60	169.9
PET fiber composite					
	125	42	1.38×10^{-0}	1.93	165.0
	127	66	5.64×10^{-1}	2.17	165.4
	130	134	8.54×10^{-2}	2.59	166.2
	132	201	3.00×10^{-2}	2.59	166.6
	135	412	4.68×10^{-3}	2.59	167.9
	137	657	1.75×10^{-3}	2.49	169.4
Aramidic fiber composite					
	125	28	3.64×10^{-0}	2.26	164.3
	127	41	1.48×10^{-0}	2.1	165.3
	130	77	3.88×10^{-1}	2.24	165.6
	132	132	9.88×10^{-2}	2.46	166.3
	135	276	1.55×10^{-2}	2.49	168.8
	137	437	3.80×10^{-3}	2.62	169.8
Sisal fiber composite					
	125	51	1.09×10^{-0}	2.77	162.8
	127	88	2.45×10^{-1}	2.73	163.6
	130	180	3.78×10^{-2}	2.64	164.7
	132	247	1.88×10^{-2}	2.55	165.9
	135	649	1.01×10^{-3}	2.74	167.9
	137	1020	2.20×10^{-3}	2.20	169.3
Glass fiber composite					
	125	44	9.45×10^{-1}	2.4	164.7
	127	70	5.09×10^{-1}	2.6	165.2
	130	152	4.26×10^{-2}	2.5	165.4
	132	238	2.79×10^{-3}	2.7	166.4
	135	509	2.15×10^{-3}	2.7	167.8
	137	820	1.06×10^{-7}	2.8	168.7

However, although the crystallization rate of PP in the blend PP–EPDM (50–50) is higher than the one observed with pure PP, it is also lower than in the blend PP–EPDM (75–25). This behavior is clearly reflected in the analysis of the half time of crystallization as a function of temperature (Fig. 3), which confirms that the increment of the PP crystallization rate is clearly higher for the blend with 25% of EPDM. This particular behavior observed on the crystallization kinetics of the blends has been explained through the balance of two opposite contributions. In first place, the results obtained suggest an increase of nucleation with the rubber content, while, on the other hand, the same rubber phase could be responsible of an impingement effect on the spherulitic growth.

Isothermal crystallization thermograms of PP in the blend (PP–EPDM 75–25), obtained at different crystallization temperatures are shown in Figure 4. It can be observed that the crystallization rate of PP in the PP–EPDM blend is strongly influenced by the crystallization temperature. This effect is still more evident when the degree of crystallization curves, obtained by integration of Figure 4 thermograms, are reported as a function of time (Fig. 5). It can be observed that an increase of 10°C in the crystallization temperature is associated with an increase of more than 10 times in the crystallization rate of the blend.

With a similar approach, isothermal tests were performed to analyze the effect of the fibers on the PP crystallization in the blends. Isothermal ther-

Table III Crystallization Parameters of PP in PP–EPDM (50–50) Blend and Its Composites

Material	T_c [°C]	$\tau_{1/2}$ [s]	K_n [min-n]	n	T_m (°C)
PP-EPDM 50-50 blend matrix					
	125	77	3.80×10^{-1}	2.36	165.6
	127	131	8.25×10^{-2}	2.70	166.1
	130	213	2.52×10^{-2}	2.61	166.4
	132	333	5.35×10^{-3}	2.83	166.3
	135	690	1.18×10^{-3}	2.61	167.8
	137	1200	4.73×10^{-4}	2.43	169.1
PET fiber composite					
	125	42	1.16×10^{-0}	1.48	164.5
	127	88	3.25×10^{-1}	1.96	165.1
	130	161	6.83×10^{-2}	2.34	165.9
	132	250	2.16×10^{-2}	2.43	166.2
	135	510	3.22×10^{-3}	2.51	167.9
	137	746	9.16×10^{-4}	2.63	169.1
Aramidic fiber composite					
	125	29	2.61×10^{-0}	1.85	163.5
	127	50	1.02×10^{-0}	2.14	163.6
	130	114	1.20×10^{-1}	2.70	165.2
	132	184	3.47×10^{-2}	2.66	166.2
	135	323	1.04×10^{-2}	2.49	167.6
	137	499	2.08×10^{-3}	2.74	168.8
Sisal fiber composite					
	125	64	5.79×10^{-1}	2.71	163.1
	127	109	1.27×10^{-1}	2.85	164.0
	130	214	2.16×10^{-2}	2.73	165.2
	132	419	2.20×10^{-3}	2.96	166.2
	135	783	4.58×10^{-4}	2.85	167.5
	137	973	5.69×10^{-4}	2.55	168.8
Glass fiber composite					
	125	62	6.54×10^{-1}	2.19	162.1
	127	106	2.02×10^{-1}	2.16	162.9
	130	147	7.93×10^{-2}	2.51	164.2
	132	248	1.14×10^{-2}	2.89	166.2
	135	530	1.43×10^{-3}	2.84	167.7
	137	809	2.97×10^{-4}	2.98	168.9

mograms and the corresponding degree of crystallization curves as a function of time of ternary composites based on the PP–EPDM (75–25) blend matrix are reported in Figures 6 and 7, respectively. From these results, it can be observed that the PP crystallization rate increases when the fibers are incorporated, i.e., all the reinforcing fibers act as nucleating agents of PP, regardless of the temperature of crystallization.

This behavior is also clearly reflected in the changes of the half time of crystallization as a function of the crystallization temperature (Fig. 8 and 9) for both PP–EPDM blend compositions. As in the case of the PP–EPDM blends, the half time increases with the crystallization temperature and, furthermore, it increases with the incorpora-

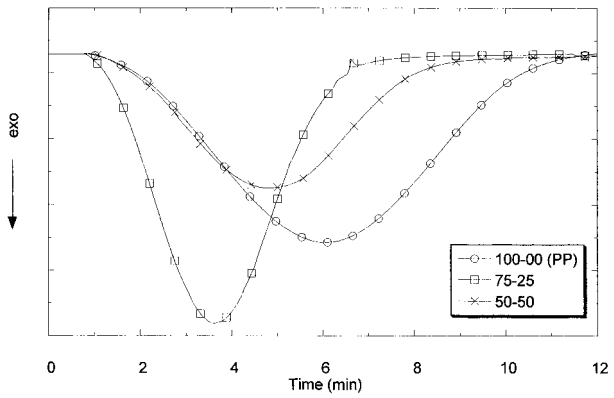

Figure 1 Isothermal crystallization thermograms of PP and PP–EPDM blends at 130°C.

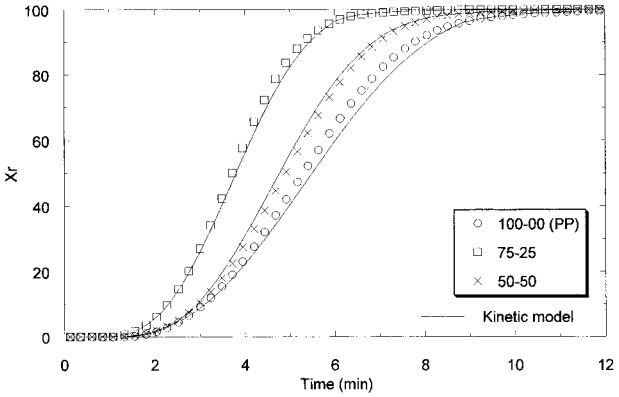

Figure 2 Degree of crystallization of PP and PP–EPDM blends at 130°C. Continuous lines represent the model predictions.

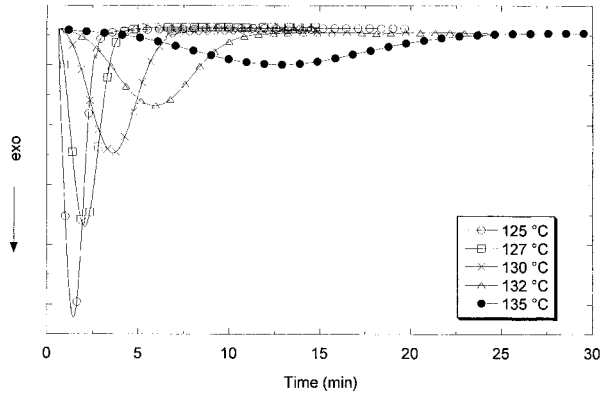

Figure 4 Crystallization isothermal thermograms of PP–EPDM (75–25) blend at different crystallization temperatures.

tion of the fibers. The half time of PP crystallization ($\tau_{1/2}$) for all the studied composites are reported in Tables II and III. Moreover, it is important to observe that similar results have been obtained in Figures 8 and 9 for both blends, suggesting that the nucleating effect of the fibers is not dependent on the blend composition.

Crystallization Kinetics

The Avrami model[28] was applied to analyze the crystallization kinetics of the studied composites accordingly with the following equation:

$$X_r(t) = 1 - \exp(-kt^n) \quad (1)$$

where X_r is the degree of crystallization obtained in isothermal crystallization experiments, n is the Avrami exponent, k is the kinetic constant, and t the crystallization time. The parameters, n and k, can be used to interpret qualitatively the nucleation mechanism, morphology, and the overall crystallization rate of the polymer. They can be calculated by plotting the results of the isothermal crystallization experiments in terms of $\log(-\ln(1 - Xr))$ vs. $\log(t)$ and evaluating the slope, which gives the Avrami exponent n, and the intercept, which gives the kinetic constant $\log k$. These logarithmic plots are reported for the PP–EPDM 50–50 reinforced with aramidic fibers in Figure 10, and have been used to calculate the Avrami parameters, n and the kinetic constant, k, of the different blends, reported in Tables II and III. In all the cases, fractional values of n were obtained, which can be explained in terms of a partial overlapping of primary nucleation and crystal growth.[29] Following the evident parallelism of Avrami plots a constant n can be assumed with an average value located in a relatively narrow

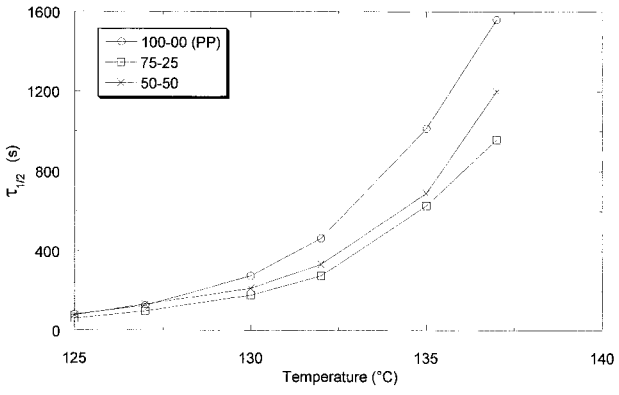

Figure 3 Half time of crystallization ($\tau_{1/2}$) vs. crystallization temperature (T_c) for PP–EPDM blends.

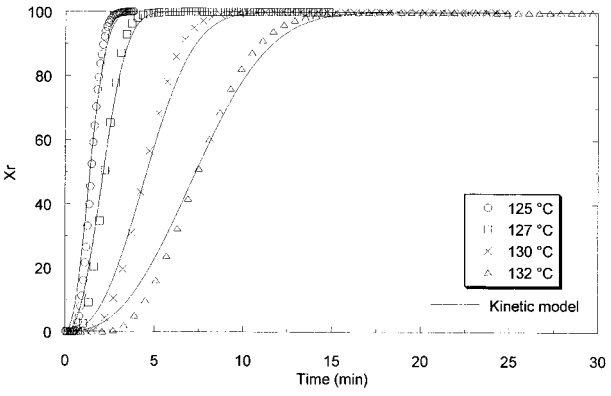

Figure 5 Degree of crystallization for PP–EPDM (75–25) blend in isothermal processes at different temperatures. Continuous lines represent the model predictions.

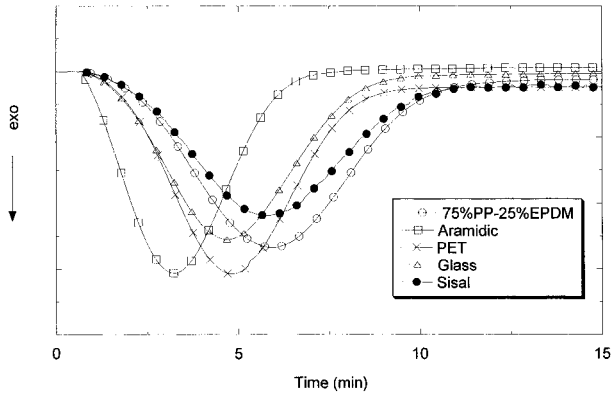

Figure 6 Crystallization isothermal thermograms of ternary composites at 130°C.

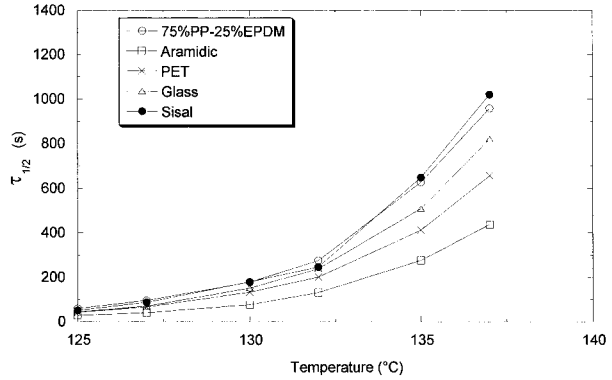

Figure 8 Half time of crystallization ($\tau_{1/2}$) vs. crystallization temperature (T_c) for ternary composites based on the PP–EPDM (75–25) blend matrix.

interval ($2 < n < 3$) traditionally attributed to a heterogeneous crystal nucleation followed by diffusion controlled spherulitic crystalline growth.

The values of the crystallization kinetic constant (k) (Tables II and III) have been normalized with the average value of n of the composites studied. These values confirm the inferred conclusions from the analysis of $\tau_{1/2}$ values. That is, the crystallization rate of the polymer matrix, PP–EPDM blends, decreases as the crystallization temperature increases, and that all the fibers act as nucleating agent for PP crystallization in PP–EPDM blends.

The ability of the model to represent the crystallization behavior of the neat polymer and of the composites is reported in Figures 2, 5, and 6, where a very good agreement between experimental and theoretical curves for isothermal processes can be easily observed. Moreover, the model developed was also used to predict the behavior of the crystallization half time as a function of the temperature during isothermal crystallization. These predictions compare well with the experimental values shown in Figure 8.

The melting temperatures of the PP–EPDM blends and of their ternary composite, determined as the maximum of the endothermic peaks obtained in DSC scans of the isothermally crystallized samples, are reported in Table II and III. The melting temperature increases as the crystallization temperature increases (Fig. 11), which is directly related to the polymer crystals size. However, T_m is not modified by the incorporation of fibers in the composite.

Nonisothermal Crystallization

The effects of the fibers on the crystallization of iPP in TPOs have also been analyzed in nonisothermal DSC experiments. Figure 12 shows the

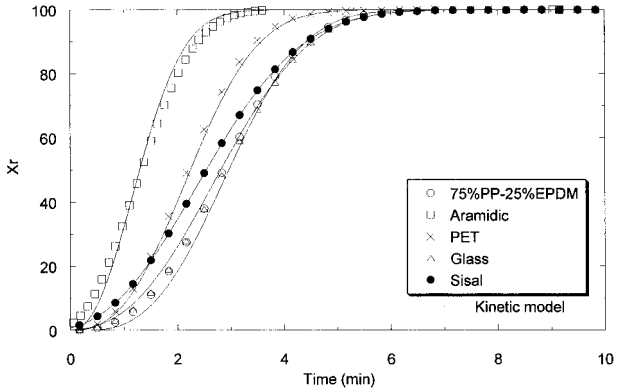

Figure 7 Degree of crystallization of PP–EPDM (75–25) blend and its composites at 130°C. Continuous lines represent the model predictions.

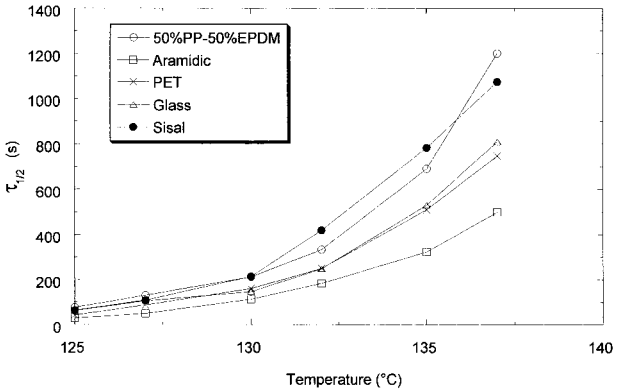

Figure 9 Half time of crystallization ($\tau_{1/2}$) vs. crystallization temperature (T_c) for ternary composites based on the PP–EPDM (50–50) blend matrix.

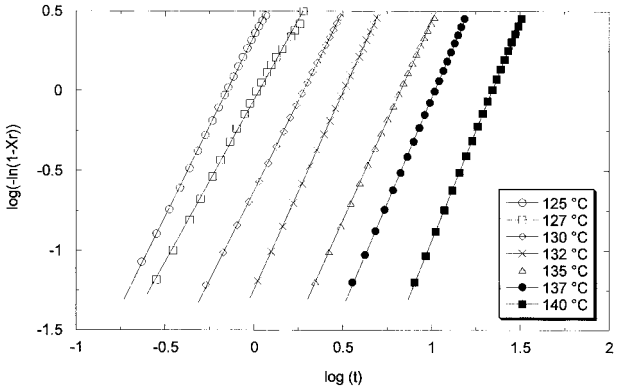

Figure 10 Avrami plots of the crystallization of PP in ternary composites based on the PP–EPDM (50–50) blend matrix with aramidic fibers.

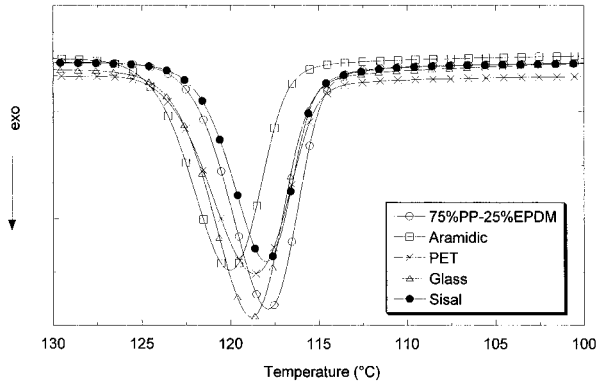

Figure 12 Crystallization dynamic thermograms of ternary composites based on the PP–EPDM (75–25) blend matrix at 10°C/min.

dynamic thermograms obtained on PP–EPDM blends and on their composites. The dynamic crystallization behavior observed confirms the results obtained in isothermal tests regarding the positive effects of the fibers studied on the crystallization kinetics of PP. The average values of the absolute degree of crystallinity (X_c), the crystallization peak (T_c), and the apparent melting temperatures of the crystallized samples (T_m) are reported in Tables IV and V.

These results show that the crystallization peak temperature decreases as the cooling rate increases while increases when fibers are incorporated in the polymer blends, this effect being more evident in the presence of the aramidic fibers. This behavior is also evident when the results are expressed in terms of the relative degree of crystallization, computed by integration of the dynamic thermograms, as reported in Figure 13

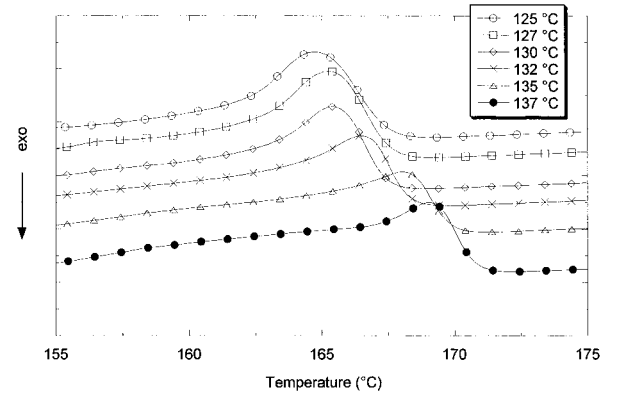

Figure 11 DSC scans at 25°C/min of PP–EPDM (50–50) blends reinforced with glass fiber after crystallization at different temperatures.

for all the composites studied. The strong nucleation ability of the fibers on PP crystallization in the blends is confirmed, and is in agreement with the results obtained in the isothermal analysis. Regarding the effect of the fibers on the melting temperature, no substantial differences were detected, while a small tendency to lower the crystallinity with the incorporation of the fibers was observed.

The dynamic crystallization analysis was also performed at different cooling rates. Complete results on the studied materials are reported in Tables IV and V. The shift in T_c with the cooling rate is directly associated to the thermal activation behavior of the crystallization process.

Spherulitic Growth Rate and Transcrystallinity

The PP spherulitic growth in the presence of both fibers and elastomer was observed by an optical polarizing microscope taking photomicrographs at different intervals of time. The spherulite formation was observed on both blend compositions and on their composites, which were melt crystallized. The main results obtained can be summarized by the fact that the PP spherulitic growth rate is influenced neither by the fibers nor by the rubber content in the blend, and only depends on the crystallization temperature utilized. These results are in agreement with the results obtained in a previous study[26] of the growth of the spherulites radius as a function of time for PP matrix/natural fiber composites, which demonstrated that the spherulitic growth rate of PP is not affected by the presence of the fibers.

The phenomenon of the transcrystallization on the fiber surface as a function of the blend matrix

Table IV Melting Temperature, Crystallinity Index, and Crystallinity Peaks of PP–EPDM (75–25) and of Its Composites Crystallized at Different Cooling Rates

	Cooling Rate: 1°C/min			Cooling Rate: 5°C/min			Cooling Rate: 10°C/min		
	T_m (°C)	X_c (%)	T_c (°C)	T_m (°C)	X_c (%)	T_c (°C)	T_m (°C)	X_c (%)	T_c (°C)
PP	164.6	36	128.9	162.4	33	121.6	161.4	32	117.9
PP + PET	164.7	32	128.4	163.0	30	122.2	162.2	29	118.7
PP + ARAMIDIC	165.3	31	130.7	163.3	29	123.6	162.9	28	120.0
PP + SISAL	164.2	25	129.2	161.9	23	121.7	160.9	22	117.9
PP + GLASS	165.9	33	130.4	163.9	30	122.8	163.1	29	118.8
	Cooling Rate: 15°C/min			Cooling Rate: 25°C/min			Cooling Rate: 50°C/min		
	T_m (°C)	X_c (%)	T_c (°C)	T_m (°C)	X_c (%)	T_c (°C)	T_m (°C)	X_c (%)	T_c (°C)
PP	160.8	31	115.3	160.2	31	111.7	159.4	30	106.1
PP + PET	161.8	28	116.1	161.2	28	112.6	160.7	28	106.9
PP + ARAMIDIC	162.5	27	117.5	162.0	27	113.8	161.2	27	107.7
PP + SISAL	160.4	22	115.7	159.9	21	113.0	159.3	21	108.5
PP + GLASS	162.6	28	115.9	162.1	24	112.1	161.4	26	105.2

composition, fiber type, and crystallization temperature was also investigated. The photomicrographs, taken at similar intervals of time during crystallization, are represented in Figures 14 and 15. In general, it was observed that independently of the fiber type, transcrystallization was enhanced by high degrees of undercooling or low crystallization temperatures. On the other hand, it was also observed that transcrystallization did not occur in the same manner with all fibers. In particular, the highest degree of transcrystallinity was obtained with aramidic fibers in the whole crystallization temperature range, whereas for PET, sisal and glass-reinforced composites transcrystallinity occurred only at high degree of undercooling.

Table V Melting Temperature, Crystallinity Index, and Crystallinity Peaks of PP–EPDM (50–50) and of Its Composites Crystallized at Different Cooling Rates

	Cooling Rate: 1°C/min			Cooling Rate: 5°C/min			Cooling Rate: 10°C/min		
	T_m (°C)	X_c (%)	T_c (°C)	T_m (°C)	X_c (%)	T_c (°C)	T_m (°C)	X_c (%)	T_c (°C)
PP	164.9	22	128.1	162.8	20	120.0	162.0	18	115.8
PP + PET	164.5	21	128.4	162.7	20	122.0	161.9	19	118.4
PP + ARAMIDIC	164.2	20	129.2	162.0	18	122.1	161.0	17	118.7
PP + SISAL	164.4	19	128.3	162.1	18	120.4	161.1	17	116.6
PP + GLASS	165.0	16	130.1	162.7	14	122.7	161.7	14	119.1
	Cooling Rate: 15°C/min			Cooling Rate: 25°C/min			Cooling Rate: 50°C/min		
	T_m (°C)	X_c (%)	T_c (°C)	T_m (°C)	X_c (%)	T_c (°C)	T_m (°C)	X_c (%)	T_c (°C)
PP	161.6	18	113.0	161.0	17	109.2	160.8	16	102.7
PP + PET	161.7	18	115.5	161.0	18	111.7	160.5	18	105.3
PP + ARAMIDIC	160.5	17	116.3	159.9	17	113.0	159.2	17	107.8
PP + SISAL	160.7	17	114.7	160.3	17	112.1	159.8	17	106.9
PP + GLASS	161.2	13	116.3	160.6	13	113.0	159.9	13	107.7

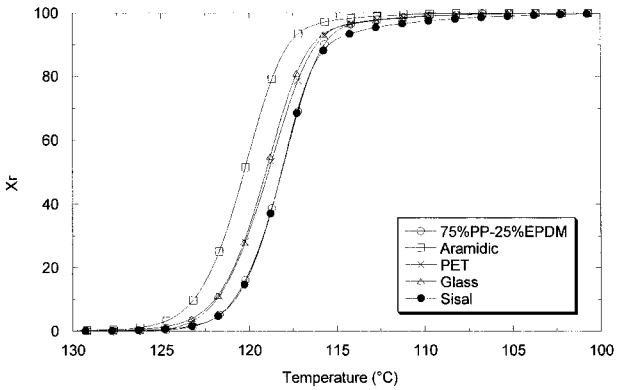

Figure 13 Degree of crystallization of PP–EPDM (75–25) blend and its composites obtained from nonisothermal crystallization experiments at 10°C/min.

When the matrix is a PP–EPDM blend, the transcrystallinity phenomenon is not favored at high rubber percentages (50%) as it is possible to observe in Figures 14 and 15. Only aramidic fibers were able to produce a small amount of transcrystallinity in the blend 50–50. While the other fibers presented a very small transcrystalline region in the PP–EPDM (75–25) blend at high degrees of undercooling, and no transcrystallinity at all at very low undercooling or in the 50–50 blend. Sisal fibers in particular did not show any transcrystallinity region for all the materials and temperatures studied.

CONCLUSIONS

Thermal analysis and optical microscopy were used to investigate the simultaneous effects of rubber ethylene–propylene–diene terpolymer (EPDM) and different kind of fibers on the crystallization and morphology of polypropylene (iPP). The kinetic study performed by DSC has demonstrated that the incorporation of both EPDM and fibers, accelerates the nucleation and crystal growth mechanisms of PP, with more marked effects at low rubber content in the blend and in the presence of the aramidic fibers. Furthermore, this nucleating effect of the fibers is not dependent on the blend composition. A good theoretical description of the crystallization behavior of PP ternary composites was obtained

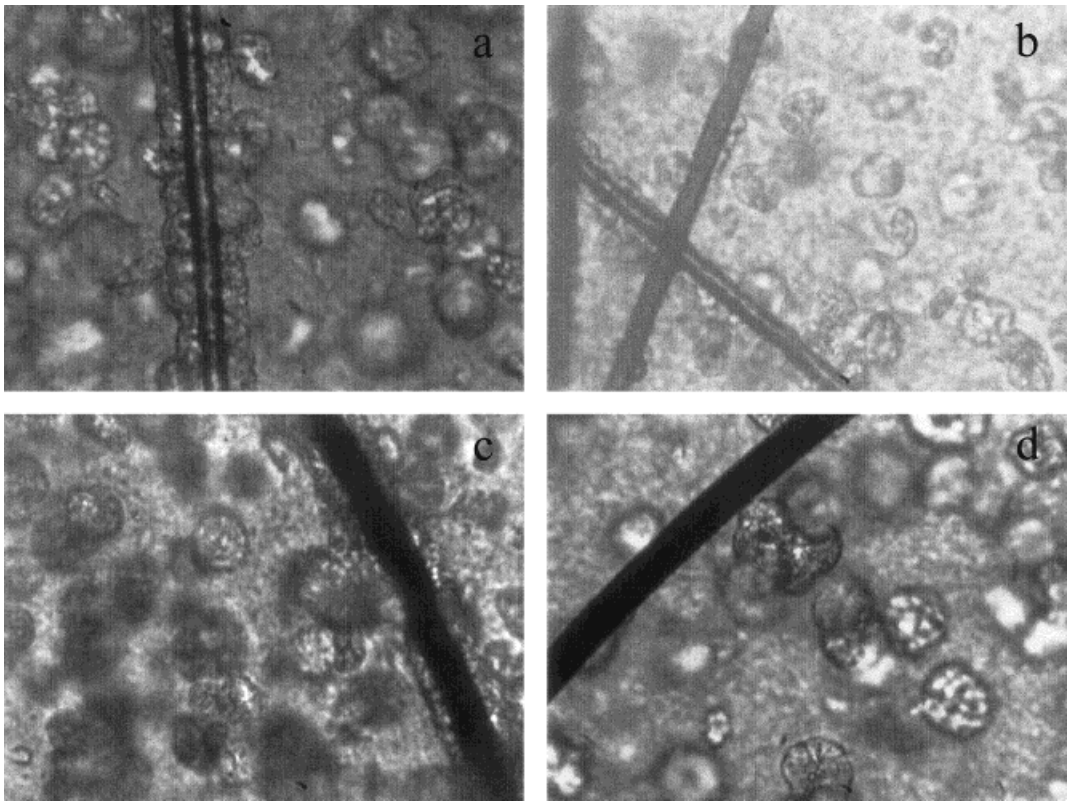

Figure 14 PP crystallization in the PP–EPDM (75–25) blend matrix in the presence of aramidic fibers at 125°C (A), 132°C (B) and PET fibers at 125°C (C) and 132°C (D).

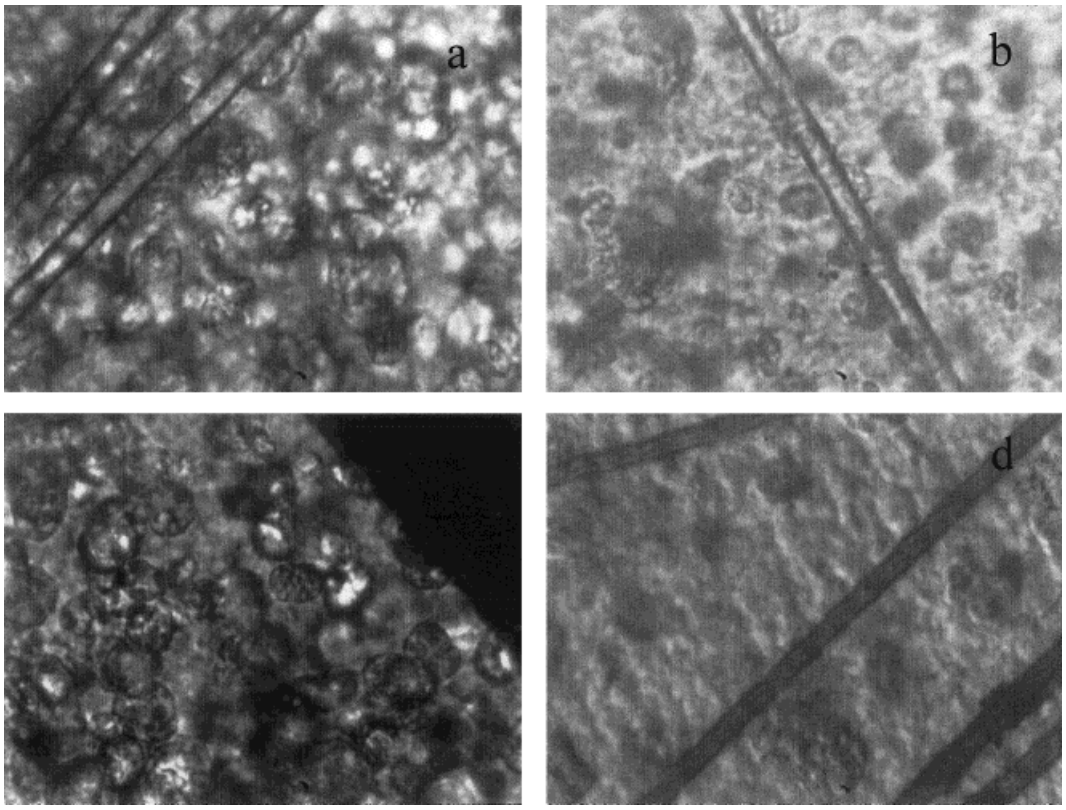

Figure 15 PP crystallization in PP–EPDM (75–25) blend in the presence of glass fibers at 125°C (A), 132°C (B), sisal fibers at 125°C (C) and PP–EPDM (50–50) blend in the presence of aramidic fibers at 125°C (D).

applying the Avrami model. Fractional values of n ($2 < n < 3$) confirmed the heterogeneous nucleation of spherulitic crystallites. In addition, the kinetic curves obtained under nonisothermal conditions provide a further confirmation of the nucleation action of both the fibers and rubber on the PP crystallization.

Microscopic analysis has revealed that transcrystallization is hindered by the presence of the elastomeric phase. Only aramidic fibers were, in fact, able to produce a small amount of transcrystallinity in the blend of 50–50. On the other hand, the rest of the fibers produced very small transcrystallinity regions in the PP–EPDM (75–25) blend at high degrees of undercooling or low crystallization temperatures.

Both DSC and microscopy studies confirmed that the fibers and the rubber behave as effective nucleant agent for the crystallization of polypropylene.

The authors wish to thank to Ministry of Education and Culture (Spain) and the Ministery of University and Scientific Research (MURST) for financial support.

REFERENCES

1. Rader, C. P. In Modern Plastics; Greene, R., Ed.; New York, 1992.
2. Thomas, D. A.; Sperling, L. K. In Polymers Blends; Newman S.; Paul, D. R., Eds.; Academic Press: New York, 1978, vol. 2.
3. Da Silva, A. N.; Tavares, M. B.; Politano, D. P.; Coutinho, F. M. B.; Rocha, M. C. J Appl Polym Sci 1997, 66, 2005.
4. Walker, B. M. Handbook of Thermoplastic Elastomers; Van Nostrand Reinhold: New York, 1979.
5. Whelan, A.; Lee, H. S. J Thermoplastic Rubbers, Appl Sci, 1982.
6. Thomas, S.; George, A. Eur Poly J 1992, 28, 1451.
7. Campbell, D. S.; Elliot, D. J.; Wheelans, M. A. N R Technol 1978, 9, 21.
8. Anon, B. Plast Rubber 1978, 32.
9. Synrott, D. J.; Sheidan, D. F.; Kontos, E. G. In Thermoplastic Elastomers from Rubber–Plastic Blends; De, S. K.; Bhowmick, A. K., Eds.; Ellis Horwood: New York, 1990.
10. Matthew, N. M.; Tinker, A. J. J Nat Rubber Res 1986, 1, 240.
11. Batiuk, M.; Harman, R. M.; Healy, J. C. US. Pat. 3,919,358, 1975 to B.F. Goodrich Co.

12. Hoppner, D.; Wendorff, J. H. Colloid Polym Sci 1990, 268, 500.
13. Karger-Kocsis, J.; Csiku, I. Polym Eng Sci 1987, 27, 241.
14. Fortelny, I.; Navratilova, E.; Kovar, J. Angew Makromol Chem 1991, 188, 195.
15. Choudhary, V.; Varma, H. S.; Varma, I. K. Polymer 1991, 32, 2541.
16. Holz, N.; Goizueta, G. S.; Capiati, N. J. Polym Eng Sci 1996, 36, 2765.
17. Campbell, D.; Qayyum, M. M. J Mater Sci 1977, 12, 2427.
18. Wunderlich, B. Makromolecular Physics; Academic Press: New York, 1976, vol. 2.
19. Folkes, M. J.; Hardwick, S. T. J Mater Sci Lett 1984, 3, 1071.
20. Peacok, J. H.; Fife, B.; Nield, E.; Barlow, C. Y. In Composites Interfaces; Ishida, H.; Koenning, J. L., Eds.; Elsevier: New York, 1986, p. 143.
21. Lee, Y.; Porter, R. S. Polym Eng Sci 1986, 26, 1574.
22. Joshi, M.; Marti, S. N.; Misra, A. Polymer 1994, 35, 3679.
23. Avalos, F.; Lopez Manchado, M.; Arroyo, M. Polymer 1998, 39, 6173.
24. Jancar, J.; Dibenedetto, A. T. J Mater Sci 1995, 30, 1601.
25. López Manchado, M. A.; Biagiotti, J.; Torre, L.; Kenny, J. J Thermal Anal Calorim, to appear.
26. López Manchado, M. A.; Biagiotti, J.; Torre, L.; Kenny, J. Polym Eng Sci, submitted.
27. Martuscelli, E.; Silvestre, G.; Abate, G. Polymer 1982, 23, 229.
28. Avrami, M. J. J Chem Phys 1939, 7, 1103.
29. Manderkern, L. Crystallization of Polymers; Mc Graw-Hill: New York, 1964.
30. Nakamura, K.; Katayama, K.; Amano, T. J Appl Polym Sci 1973, 17, 1031.